



Performance of semi-insulating gallium arsenide X-ray pixel detectors with current-integrating readout

P.J. Sellin^{a,*}, G. Rossi^b, M.J. Renzi^b, A.P. Knights^d, E.F. Eikenberry^c,
M.W. Tate^b, S.L. Barna^b, R.L. Wixted^e, S.M. Gruner^b

^a *Department of Physics, University of Surrey, Surrey, Guildford GU2 7XH, UK*

^b *Cornell University, LASSP, Ithaca, NY 14853-2501, USA*

^c *Department of Pathology, UMDNJ-Robert Wood Johnson, Piscataway, NJ 08854, USA*

^d *Department of Electronic and Electrical Engineering, University of Surrey, Guildford GU2 5XH, UK*

^e *Department of Physics, Princeton University, Princeton, NJ 08544, USA*

Abstract

First images are presented from tests of a semi-insulating gallium arsenide X-ray imaging detector, flip-chip bonded to a current integrating CMOS readout chip. The detector is designed for applications in synchrotron X-ray imaging. The X-ray sensing part of the detector consists of a 150 μm thick GaAs photodiode containing an array of 92×100 pixels, each 150 μm by 150 μm in size. Operating the device at -20°C we have obtained a map of detector dark current, which is typically in the range 0.4 pA to 0.8 pA/pixel. We have also obtained images of the detector response to a collimated X-ray beam. © 2001 Elsevier Science B.V. All rights reserved.

1. Introduction

We report the first results from a gallium arsenide (GaAs) X-ray imaging detector that has been designed for applications in synchrotron X-ray imaging, as part of the Cornell University Pixel Array Detector (PAD) program. The PAD detector concept consists of a current-integrating pixel readout CMOS chip, flip-chip bonded to a pixellated semiconductor photodiode, and has been previously described in Ref. [1]. This type of current-integrating readout architecture is well suited for ultra-high rates of incident photons, although other types of photon-counting based imaging detectors are also under development for possible synchrotron X-ray imaging applications

[2]. In a flip-chip bonded hybrid detector the technology of the readout chip can be separated from that of the X-ray conversion layer, which typically consists of a pixellated photodiode fabricated from high resistivity silicon or a high atomic number compound semiconductor such as GaAs. In contrast to CCD-based X-ray detectors that have been previously developed for synchrotron X-ray imaging [3] the X-ray conversion layer in a hybrid detector has a sufficient active thickness to detect X-ray photons directly with a high efficiency. A previous, smaller version of the PAD detector readout chip has already been successfully characterised, connected to a silicon photodiode array [4]. In this paper we report on the first data obtained with a GaAs photodiode bonded to a full size 92×100 pixel PAD readout chip. Evaluation of the CMOS chip

*Corresponding author.

bump bonded to a silicon photodiode is reported in Ref. [5].

GaAs photodiodes are of particular interest for X-ray imaging detectors due to their improved photon detection efficiency compared to silicon photodiodes of comparable thickness. Detectors fabricated from GaAs have a linear attenuation coefficient for X-ray photons similar to that of germanium but are able to operate at, or close to, room temperature. As the next generation of synchrotron sources moves towards increasing beam energies, there is a requirement for new X-ray imaging technologies suitable for higher energy photon detection. The use of GaAs as the photodiode material in this type of hybrid detector offers the combined advantages of greater photon detection efficiency plus greater radiation shielding of the potentially sensitive CMOS readout chip.

Semi-insulating bulk GaAs has been extensively developed as a material for radiation detection, most recently for X-ray imaging devices. A comprehensive review of the detection properties of the material can be found in Ref. [6]. Pixellated GaAs imaging detectors are currently being developed for applications outside of synchrotron radiation, for example for use in mammographic X-ray imaging [7]. Semi-insulating GaAs is widely available in wafers of suitable thickness (typically 100–600 μm) and has a resistivity of $\sim 10^7 \Omega\text{cm}$. The high resistivity is obtained through a compensation mechanism involving both deep level and shallow traps, which can cause short carrier lifetimes leading to incomplete charge collection at the detector electrodes. The charge collection efficiency observed in semi-insulating GaAs radiation detectors has been found to be highly material-specific, and correlated to the concentration of the ionised EL2^+ mid band-gap trap [8,9]. Depending on material quality, charge collection efficiencies for semi insulating GaAs detectors of 200 μm thickness have been reported within the range 30–90%. The presence of possible inhomogeneity across the GaAs wafer, which could cause regions of poor charge collection or high leakage current, is of importance particularly for an imaging detector using a current-integrating architecture. The detectors used in this work were fabricated from GaAs produced using the “vertical

gradient freeze” (VGF) technique¹ which has been reported to show improved homogeneity compared to wafers produced by the ‘liquid encapsulated czochralski’ (LEC) method [10].

2. Experimental method

The GaAs photodiodes were fabricated at the University of Surrey using 150 μm thick 2 inch diameter wafers of VGF GaAs. Pixellated Schottky contacts were produced on the front surface of the device using standard thermal evaporation and lift-off techniques. Each device consisted of an array of 92×100 pixels, arranged on a 150 μm square pitch. The inter-pixel gap was 20 μm and a single guard ring was used to enclose the complete array. A uniform ohmic contact was deposited over the whole rear surface of the wafer, and ion beam implantation of the ohmic contact was used to improve the high voltage stability of the device.

The CMOS readout chip was designed with an on-chip frame storage capability for microsecond time-resolved experiments. The device is capable of storing up to 8 sequential frames with microsecond time resolution before data readout and has an adjustable exposure time ranging from 1 μs up to many seconds. The CMOS chip was fabricated by the MOSIS service² using a Hewlett-Packard 1.2 μm CMOS process and was bump bonded to the GaAs photodiode layer by GEC-Marconi³. Each pixel readout channel contains an integrating input amplifier, an array of 8 storage capacitors and an output amplifier. The integration time is externally selectable using a logic gate pulse of duration from 1 μs up to several minutes, although the practical upper limit for integration time is set by the leakage current of the pixel diode. The minimum time between two successive frames (400 ns) is limited in the present design by the time required to reset the integration capacitor in the input stage.

¹Supplied by American Xtal Technology (AXT), Fremont, CA, USA

²The MOSIS Service, Information Sciences Institute, University of Southern California, Marina del Rey, CA, USA.

³Marconi Materials Technology, Caswell, UK.

The complete detector was wire bonded to a PCB motherboard and mounted inside a vacuum cryostat. An aperture in the centre of the PCB allowed the back of the pixel detector to be thermally connected to a peltier cooler which cooled the detector during operation to -20°C . A light-tight polymer/aluminum composite window is mounted in the cryostat end plate in front of the detector, allowing X-rays to reach the device. A complete description of the experimental arrangement and performance of the 92×100 CMOS chip has been published elsewhere [4,5].

3. Results and discussion

An important aim of these detector studies was to assess the dark current produced by semi-insulating GaAs photodiodes when operated at reduced temperature. We have previously measured the reduction in dark current in semi-insulating GaAs detectors due to cooling, using simple 3 mm diameter circular pad detectors fabricated from similar VGF material. For 200 μm thick pad detectors we observed a significant reduction in detector leakage current, from approximately $5 \times 10^{-9} \text{ A/mm}^2$ at $+20^{\circ}\text{C}$ to a value of approximately $2 \times 10^{-10} \text{ A/mm}^2$ at a temperature of -20°C .

In the GaAs PAD the thermally generated dark current within the diode layer provided a source of stable, uniform current useful for characterisation of the detector performance. The devices were also characterised with X-rays using a conventional laboratory generator. In both cases the detector was biased at -100 V and operated in a light tight cryostat at a temperature of -20°C .

3.1. Dark current images

In the absence of any X-ray radiation, images were acquired from the detector by integrating the thermally generated dark current of the GaAs photodiode layer with an integration time from 25 to 600 ms. For each integration time value, an average value of the dark image pixel signal was calculated in each image by taking the mean signal from a single row of pixels. This is plotted as a

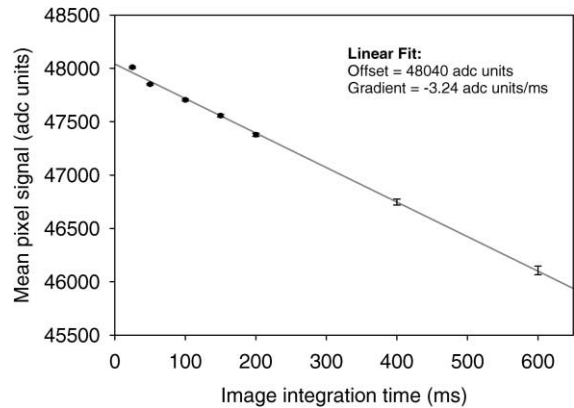


Fig. 1. Plot of mean pixel signal due to detector dark current vs image integration time. The data are fitted by a linear function, giving a pixel baseline value at zero integration time of 48 040 ADC units.

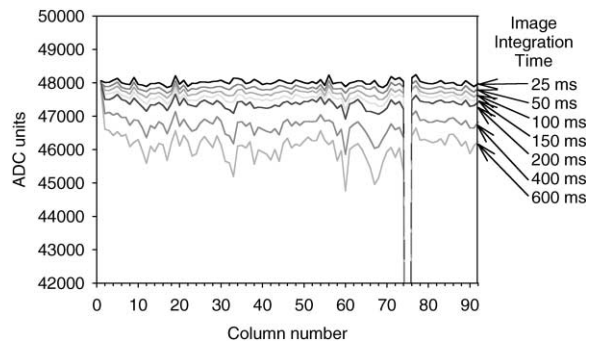


Fig. 2. Profile of a single row of pixels from a number of raw data images, acquired with different image integration times. The saturated pixels in columns 74 and 75 are due to a readout problem in the detector (see text).

function of image integration time in Fig. 1. Since the CMOS integrating electronics was devised for hole collection, upon integration of positive charge on the current integrating amplifier feedback capacitor, the output voltage of the integrating amplifier is expected to swing towards zero volts from its initial baseline value. The downward integration action is shown in Fig. 1 for the dark current data: the average pixel signal was extrapolated to zero integration time, and gave an average pixel DC baseline of 48 040 ADC units (the DC bias voltage of the integrating amplifier), or 3.66 V.

Fig. 2 shows profiles of raw image data taken from a single row in the detector, as a function of

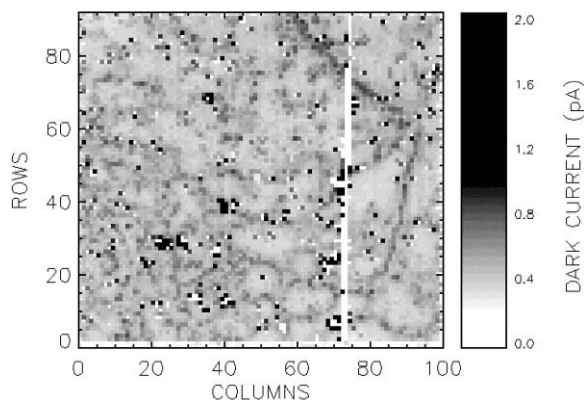


Fig. 3. Computed map of dark current of the GaAs PAD detector at a bias of -100 V and operating at a temperature of -20°C . The typical pixel dark currents in the regions of uniform response are between 0.4 pA and 0.8 pA/pixel.

image integration time. The saturated pixels in columns 74–75 (see below) are clearly visible with ADC values outside the displayed scale. At an integration time of 50 ms the mean pixel signal is 47850 ADC units. After baseline subtraction this gives a net average integrated signal of 190 ADC units with a standard deviation of 79 ADC units.

Fig. 3 shows a computed dark current map of the array of GaAs photodiode pixels. It was computed using the set of dark current images collected at different integration times: the fitted slope of Fig. 1 (ADC units of integrated signal variation over integration time) is proportional to the integrated dark current and the integration capacitor, for which a 2 pF nominal value was used. This map contains 100 columns by 92 rows, and contains uniform pixel values over the majority of the image. There is a clearly visible dead vertical stripe on the right hand side of the image, corresponding to columns 74–75. The exact nature of this defect is still under investigation. The dark current map shows a mean pixel leakage current, in the regions of uniform response, of between 0.4 pA and 0.8 pA/pixel, corresponding to a current density of 1.7×10^{-11} to 3.6×10^{-11} A/mm². Various regions of variation in the leakage current within this range are visible in the image, appearing both as circular patterns and also as linear regions and corresponding to regions of different resistivity within the GaAs material.

The dark current map also shows several randomly distributed artefacts, particularly a number of dark multi-pixel spots in the image located in the bottom left region of the image. A typical cluster is located at row 35 column 23. These clusters correspond to hot spots of high leakage current within the GaAs material. Unlike the regions of small variation in background current discussed above, these clusters appear only at higher detector bias voltages and are most likely associated with the onset of breakdown within the GaAs.

The image also shows a number of two-pixel artefacts, quite different in type to the hot clusters described above. These features always consist of a pair of adjacent pixels in which the charge collected from one pixel is always above the average pixel value whilst the charge collected from the other pixel in the pair is always below the average, by approximately equal magnitudes. The cause of these features is most likely due to localised bump bonding defects, consistent with similar defects observed in a considerably smaller proportion of other detectors bump-bonded to silicon photodiodes. It should be remembered that GaAs and silicon have quite different coefficients of thermal expansion, introducing a higher mechanical strain during detector cooling at the bump-bond level when compared to the case in which a silicon diode layer is used.

Using the multiple-image storage capacity of the PAD readout chip, eight dark current images could be acquired at a fixed integration time, with only a 2 μs dead time between each image. This feature of the device was used to investigate possible dynamic fluctuations in the response of the GaAs photodiode. The presence of fluctuating current pulses in semi-insulating GaAs radiation detectors has been reported elsewhere [11] and recently there have been reports of fluctuating hot spots observed in semi-insulating GaAs pixel array detectors [12]. In order to search for such effects we collected eight successive images, each with a 25 ms image integration time and separated by a 2 μs deadtime. At a detector bias of 100 V we observed no significant fluctuations between the eight images for a given region of pixels. Similarly, no significant fluctuations were observed when eight

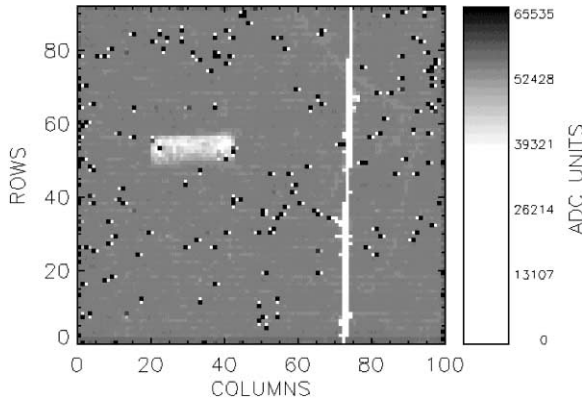


Fig. 4. A raw image from the GaAs PAD detector irradiated with a collimated rectangular beam of 8.9 keV X-rays from a laboratory X-ray generator. The image integration time is 500 ms.

images were acquired with 400 ms integration times, again with a 2 μ s deadtime between each image.

3.2. X-ray images

The performance of the GaAs detector under irradiation was measured using X-rays produced by an Enraf–Nonius copper anode X-ray tube operated at 20 kV. A monochromator was used to select photons from the K_{β} line with an energy of 8.9 keV, which were then collimated using a set of slits to illuminate a small, approximately rectangular region of the GaAs detector. Fig. 4 shows a single raw data image obtained from the irradiated detector with an image integration time of 0.5 s. The majority of the surface area of the detector was not irradiated by the X-rays, and showed a typical pixel signal of approximately 47 000 ADC units, somewhat different from the reported value measured with the dark current since a slightly different bias of the integrating amplifier was used. The irradiated portion of the detector is clearly visible in the centre left region of the image with a typical pixel raw signal in the irradiated region of approximately 35 000 ADC counts. It should be remembered that in the PAD readout system the ADC output swings towards zero with increasing pixel signal.

Fig. 5 shows the same data after subtraction of a background image acquired under identical conditions but in the absence of X-ray photons.

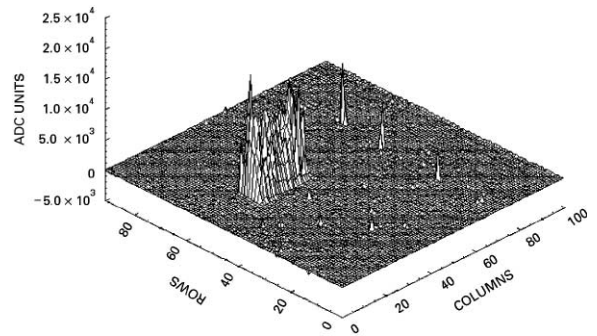


Fig. 5. The X-ray image from the GaAs PAD detector after background subtraction. The rectangular area of pixels illuminated by the collimated X-ray beam is clearly visible towards the centre of the image.

Subtraction of the background image clearly improves the image quality by removing the various artefacts such as those due to bump-bonding problems. The uniformity of the pixel signals in the region of the detector that has been irradiated with X-rays appears to be relatively poor due primarily to nonuniformity in the X-ray beam.

The pixel well depth was measured for those pixels which reached saturation upon integration of the X-ray signal. An average pixel well depth of 42 000 ADC units was computed. Using the measured dark current reported in the previous section, the saturation time of the sensor due to dark current is more than 10 seconds.

4. Conclusion

We have conducted some first tests on a semi-insulating GaAs pixel detector fabricated from 150 μ m thick VGF GaAs. The GaAs photodiode was bump-bonded to a CMOS readout chip operating in a current-integrating mode. The test detector consisted of a single array of 92 \times 100 pixels, each pixel having a size of 150 \times 150 μ m. The dark current observed when operating the detector at a temperature of -20°C is approximately 0.4–0.8 pA/pixel, which is well within the limit required for successful operation of this device. Images of the detector dark current obtained for a range of image integration times between 25 and 600 ms

showed evidence for zones of lower resistivity within the GaAs material.

The raw data images also contained a number of artefacts, primarily consisting of pairs of pixels with non-uniform signal response. These are attributed to problems with the bump bonding between the GaAs and CMOS layers. A small number of “hot spots” were also observed in the raw images, consisting of clusters of several pixels with an abnormally high signal level. These are possibly due to the onset of detector breakdown of the GaAs photodiode.

A preliminary investigation was also made of the response of the detector to irradiation with 8.9 keV photons, using an image integration time of 0.5 s. The profile of the highly collimated X-ray beam could be clearly observed against the background signal, and the quality of the image was further improved by subtraction of a background image.

Further work is in progress to improve the quality and uniformity of the GaAs signal response and dark current characteristics, and to reduce the number of faulty pixels caused by the bump-bonding process.

Acknowledgements

This work was funded under US Department of Energy grants DE-FG-0297ER14805 and DE-FG-0297ER62443. Author P.S. acknowledges funding from the UK Biotechnology and Biological Sciences Research Council under grant number 50/X08150.

References

- [1] E.F. Eikenberry, S.L. Barna, M.W. Tate, G. Rossi, R.L. Wixted, P.J. Sellin, S.M. Gruner, *J. Synchrotron Radiat.* 5/3 (1998) 252.
- [2] S. Manolopoulos, R. Bates, G. Wye, M. Campbell, G. Derbyshire, R. Farrow, E. Heijne, V. O’Shea, C. Raine, K.M. Smith, *J. Synchrotron Radiat.* 6 (1999) 112.
- [3] M.W. Tate, E.F. Eikenberry, S.L. Barna, M.E. Wall, J.L. Lowrance, S.M. Gruner, *J. Appl. Crystallogr.* 28 (1995) 196.
- [4] S.L. Barna, J.A. Shepherd, M.W. Tate, R.L. Wixted, E.F. Eikenberry, S.M. Gruner, *IEEE Trans Nucl. Sci.* 44/3 (1997) 950–956.
- [5] G. Rossi, M. Renzi, E.F. Eikenberry, M.W. Tate, D. Bilderback, E. Fontes, R. Wixted, S. Barna, S.M. Gruner, *J. Synchrotron Radiat.* 6 (6) (1999) 1096.
- [6] D.S. McGregor, H. Hermon, *Nucl. Instr. Meth. A* 395 (1997) 101.
- [7] S.R. Amendolia, E. Bertolucci, M.G. Bisogni, U. Bottigli, M.A. Ciocci, M. Conti, P. Delogu, M.E. Fantacci, G. Magistrati, V. Marzulli, E. Pernigotti, N. Romeo, V. Rosso, P. Russo, A. Stefanini, S. Stumbo, *Nuovo Cimento A – Nuclei Part. Fields* 112 (1999) 167.
- [8] K. Berwick, M.R. Brozel, C.M. Buttar, J.S. Pooni, P.J. Sellin, S.M. Young, *Nucl. Instr. and Meth. A* 380 (1996) 46.
- [9] M. Rogalla, R. Geppert, R. Goppert, M. Hornung, J. Ludwig, Th. Schmid, R. Irsigler, K. Runge, A. Soldner-Rembold, *Nucl. Instr. and Meth. A* 410 (1998) 74.
- [10] D.S. McGregor, H.C. Chui, J.E. Flatley, R.L. Henry, P.E.R. Nordquist, R.W. Olsen, M. Pocha, C.L. Wang, *Nucl. Instr. and Meth. A* 380 (1996) 165.
- [11] K. Berwick, M.R. Brozel, *IOP Conference Series* 160 (1997) 123.
- [12] R. Irsigler, J. Andersson, J. Alverbro, J. Borglind, C. Fröjd, P. Helander, S. Manolopoulos, V. O’Shea, K. Smith, *Nucl. Instr. and Meth. A* 434 (1999) 24.